

Neutron resonance spectroscopy: $^{175}\text{Lu}^\dagger$

H. I. Liou, J. Rainwater, G. Hacken, and U. N. Singh

Columbia University, New York, New York 10027

(Received 27 November 1974)

Results are given of high resolution measurements of the neutron resonance parameters (E_0 , $g\Gamma_n^0$) for 446 resonances to 3 keV in ^{175}Lu using the Columbia University Nevis synchrocyclotron. The measurements used the 202.05 m flight path for transmission measurements and the 39.57 m flight path for transmission, capture, and self-indication measurements. Values of Γ_γ from (59 ± 20) to (100 ± 20) meV were obtained for 40 levels, with $\langle \Gamma_\gamma \rangle = 77$ meV. The s wave strength function is $10^4 S_0 = (1.83 \pm 0.12)$ and the deduced mean s level spacing is (3.45 ± 0.15) eV. Using recent unpublished J assignments for levels below 238 eV by Namenson, Stolovy, and Smith, we obtain (0.55 ± 0.20) for the ratio of the $J = 4$ to $J = 3$ s strength functions. The results to 200 eV agree with values expected from the orthogonal ensemble theory for level spacing systematics.

[NUCLEAR REACTIONS $^{175}\text{Lu}(n, n)$, (n, γ) , $E = 1 \text{ eV} - 3 \text{ keV}$; measured $\sigma_t(E)$; deduced E_0 , $g\Gamma_n^0$, Γ_γ , S_0 , $\langle D_0 \rangle$, $S_0(J=4)/S_0(J=3)$; various statistical tests.]

I. INTRODUCTION

This is one of a series¹⁻¹⁷ of papers reporting the results of high resolution neutron time of flight spectroscopy measurements using the Columbia University Nevis synchrocyclotron. We report the results of 202.05 m path transmission measurements and 39.57 m path capture, self-indication, and transmission measurements on samples of Lu_2O_3 enriched to 99.926% in ^{175}Lu . The samples were suitable for establishing the resonance parameters (E_0 , $g\Gamma_n^0$) for 446 levels in ^{175}Lu to 3 keV, but were too thin to obtain the total cross section behavior between resonances. This nuclide falls in the region of a split maximum of the $l=0$ strength function and has a small average s level spacing, $\langle D \rangle \approx 3.45$ eV. A Bayes's theorem analysis of our data indicates that it is quite improbable that any $l=1$ levels could have been included even if $10^4 S_1$ were as high as 4, which itself is very unlikely. Below 500 eV we were able to obtain values for the neutron capture widths for 40 levels. ^{175}Lu has the binding energy for an extra neutron = 6.293 MeV.

The s levels in ^{175}Lu ($J^\pi = \frac{7}{2}^+$) are expected to form two nearly equal abundant populations having $J=3$ and 4 for the compound nucleus. We have not determined favored J values for any of the resonances, since the two possible spin weight factors $g = \frac{7}{16}$ or $\frac{9}{16}$ are nearly equal. We obtain $g\Gamma_n^0$ for the "strength" of each level. The samples are sufficiently pure isotopically that only ^{175}Lu levels are included.

The main results for Lu by other experimenters are those of Block, Slaughter, and Harvey¹⁸ (ORNL) who obtained level parameters for 16 resonances in ^{175}Lu to 57.4 eV and 20 levels in ^{176}Lu

to 46.7 eV using a sample enriched to 70.2% ^{176}Lu . In addition, Harvey, Hughes, Carter, and Pilcher (BNL)¹⁹ obtained parameters for 33 resonances in natural Lu (97.4% ^{175}Lu , 2.6% ^{176}Lu) to 132 eV. Above 57.5 eV, the BNL measurements do not properly resolve levels so no useful comparison can be made with our results. Both the ORNL and BNL groups resolved most ^{175}Lu levels below 57.5 eV. Only level energies for our preliminary results to 1201.5 eV are included in the 1973 edition of BNL-325.²⁰ Wasson and Chrien²¹ reported σ_γ (spectra) measurements to 40.6 eV. Recently, Namenson, Stolovy, and Smith,²² (Naval Research Laboratory) have reported the results of capture γ ray spectra measurements emphasizing the ratios of the strengths of particular γ ray transition that are differently favored for $J=3$ or 4. Their results favored $J=3$ for 29 levels and $J=4$ for 28 levels in ^{175}Lu to 274 eV. In most cases, they calculate that there is >90% probability that their J assignment is correct.

We use their results to make further statements concerning the $J=3$ and 4 s level populations using our $g\Gamma_n^0$ values at levels where they establish J . The detailed analysis of our data for ^{175}Lu resonance parameters is mainly due to Dr. Liou.

II. EXPERIMENTAL DETAILS AND PRELIMINARY RESULTS

The data for ^{175}Lu were obtained during the same cyclotron "run" as for the Er,¹ Yb,⁴ Sm,² Eu,² W,⁵ and In,⁹ isotopes. The conditions for the cyclotron operation, flightpaths, and time of flight analyzer have been described in Ref. 1. The 202.05 m transmission measurements used only the thicker sample having $1/n = 70.4$ b/atom of

TABLE I. Resonance energies and $g\Gamma_n^0 = g\Gamma_n(1 \text{ eV}/E)^{1/2}$ values for the levels in ^{175}Lu .

E_0 (eV)	$g\Gamma_n^0$ (meV)	E_0 (eV)	$g\Gamma_n^0$ (meV)	E_0 (eV)	$g\Gamma_n^0$ (meV)	E_0 (eV)	$g\Gamma_n^0$ (meV)
2.590+0.005	0.062+0.004	265.05+0.30	0.029+0.006	587.92+0.39	0.64 +0.09	922.1+0.4	1.9 +0.3
4.753+0.012	0.064+0.009	267.88+0.31	0.022+0.009	592.63+0.40	0.32 +0.05	928.8+0.4	1.3 +0.3
5.200+0.026	0.30 +0.04	273.70+0.32	2.2 +0.2	597.00+0.40	1.4 +0.2	930.8+0.4	0.19+0.07
11.20 +0.02	0.45 +0.03	277.70+0.26	0.35 +0.04	601.42+0.41	0.65 +0.12	940.0+0.4	2.4 +0.4
13.97 +0.03	1.9 +0.3	282.21+0.26	0.26 +0.03	605.27+0.41	3.7 +0.6	943.7+0.4	1.5 +0.3
15.31 +0.03	0.22 +0.03	288.70+0.27	2.2 +0.3	614.76+0.42	1.7 +0.3	950.1+0.8	0.08+0.04
20.45 +0.03	0.21 +0.02	291.52+0.27	2.0 +0.3	621.28+0.43	1.5 +0.2	954.6+0.4	0.22+0.08
23.42 +0.03	0.50 +0.04	294.90+0.28	0.93 +0.12	625.54+0.43	0.18 +0.07	960.0+0.4	1.5 +0.2
27.92 +0.04	0.15 +0.01	298.83+0.36	0.024+0.012	627.26+0.43	5.0 +0.8	964.7+0.4	2.0 +0.4
30.11 +0.05	0.66 +0.05	304.48+0.29	0.56 +0.07	630.28+0.44	0.10 +0.05	968.2+0.4	0.87+0.19
31.01 +0.05	0.25 +0.04	307.70+0.30	0.18 +0.02	633.25+0.44	0.56 +0.08	974.2+0.4	0.61+0.10
36.50 +0.06	0.51 +0.03	314.01+0.31	1.4 +0.1	638.75+0.44	0.32 +0.06	984.3+0.4	0.36+0.10
40.59 +0.07	1.6 +0.3	317.08+0.31	0.48 +0.10	644.38+0.45	0.075+0.024	986.8+0.4	0.35+0.13
41.06 +0.07	0.11 +0.04	318.32+0.31	1.5 +0.3	648.88+0.45	1.8 +0.3	989.4+0.4	1.2 +0.3
49.40 +0.05	0.77 +0.07	322.72+0.32	0.24 +0.04	654.35+0.46	1.6 +0.3	1004.9+0.5	0.22+0.08
50.27 +0.05	0.56 +0.06	324.40+0.32	0.13 +0.02	657.57+0.46	2.0 +0.4	1008.4+0.5	2.0 +0.3
53.54 +0.06	0.029+0.003	330.20+0.33	5.4 +0.6	666.90+0.47	0.19 +0.05	1012.4+0.5	0.38+0.06
57.01 +0.06	0.33 +0.03	338.34+0.34	0.48 +0.07	671.16+0.48	0.97 +0.15	1023.5+0.5	0.28+0.06
61.18 +0.06	0.028+0.003	340.74+0.35	0.20 +0.03	676.91+0.48	0.44 +0.07	1027.8+0.5	0.58+0.12
69.50 +0.07	0.053+0.011	343.60+0.35	1.3 +0.2	681.76+0.49	0.84 +0.11	1034.8+0.5	0.97+0.16
69.99 +0.07	0.12 +0.02	347.91+0.36	1.3 +0.2	686.17+0.49	1.1 +0.2	1043.2+0.5	6.2 +1.1
73.70 +0.09	0.010+0.002	355.87+0.37	0.27 +0.04	692.61+0.50	1.8 +0.3	1050.5+0.5	0.31+0.11
81.12 +0.10	0.014+0.001	358.75+0.37	0.43 +0.06	696.63+0.51	0.14 +0.05	1055.1+0.5	1.2 +0.3
85.50 +0.06	0.42 +0.03	364.22+0.38	0.084+0.010	699.15+0.51	0.35 +0.09	1059.1+0.5	1.0 +0.2
88.56 +0.06	0.28 +0.02	367.16+0.39	0.14 +0.02	705.00+0.51	0.79 +0.11	1063.2+0.5	0.40+0.09
96.69 +0.14	3.3 +0.4	379.45+0.41	0.82 +0.10	710.95+1.32	0.068+0.026	1066.5+0.5	1.4 +0.3
99.74 +0.07	0.55 +0.05	383.07+0.41	0.51 +0.10	717.85+0.53	1.3 +0.2	1079.3+0.5	0.26+0.05
100.84 +0.07	0.30 +0.03	385.25+0.42	0.19 +0.03	723.56+0.53	0.74 +0.15	1085.3+0.5	0.67+0.12
103.00 +0.08	0.51 +0.04	393.32+0.43	4.0 +0.5	725.70+0.54	1.6 +0.3	1091.7+0.5	4.8 +0.9
107.45 +0.08	1.6 +0.2	398.29+0.44	0.28 +0.04	735.98+0.55	0.17 +0.05	1103.2+0.5	0.75+0.12
112.94 +0.13	0.15 +0.02	405.35+0.45	1.7 +0.2	739.60+0.55	0.74 +0.11	1109.7+0.5	1.4 +0.3
115.24 +0.18	1.7 +0.2	413.05+0.46	0.20 +0.03	750.40+0.56	1.1 +0.2	1113.3+0.5	1.3 +0.3
118.69 +0.09	0.67 +0.09	418.98+0.24	0.81 +0.08	753.60+0.57	0.60 +0.11	1118.4+0.5	0.21+0.07
119.45 +0.09	0.057+0.014	422.28+0.24	0.15 +0.02	758.92+0.57	0.094+0.033	1122.0+0.5	0.27+0.09
124.45 +0.10	0.011+0.005	428.04+0.24	0.24 +0.03	761.21+0.58	0.43 +0.07	1129.7+0.5	0.89+0.30
127.37 +0.10	1.6 +0.2	434.17+0.25	1.3 +0.1	767.87+0.58	2.3 +0.3	1131.5+0.5	1.5 +0.5
129.61 +0.11	2.2 +0.3	438.92+0.25	0.57 +0.10	774.32+0.59	0.20 +0.04	1138.2+0.5	0.53+0.09
137.88 +0.11	1.3 +0.1	440.05+0.26	0.62 +0.10	777.30+0.60	0.86 +0.14	1143.9+0.6	0.53+0.12
143.05 +0.12	0.14 +0.02	444.00+0.26	1.3 +0.1	783.30+0.61	0.45 +0.07	1146.5+0.6	0.27+0.12
146.33 +0.13	0.21 +0.02	450.90+0.67	0.056+0.014	791.41+0.61	0.32 +0.09	1153.0+0.6	4.4 +0.7
148.65 +0.13	0.090+0.008	454.42+0.27	0.39 +0.06	794.47+0.62	0.46 +0.11	1164.8+0.6	4.1 +0.7
151.02 +0.13	0.16 +0.02	457.21+0.69	0.051+0.014	796.62+0.62	0.92 +0.21	1175.2+0.6	3.5 +0.7
155.56 +0.14	0.23 +0.02	467.15+0.28	0.36 +0.07	801.26+0.63	0.49 +0.11	1180.0+0.6	1.3 +0.3
158.49 +0.14	0.43 +0.04	468.82+0.28	0.26 +0.05	803.41+0.63	3.5 +0.7	1186.1+0.6	0.90+0.17
163.80 +0.15	0.47 +0.04	473.58+0.28	1.2 +0.2	818.29+0.64	0.16 +0.04	1201.9+0.6	0.32+0.09
169.28 +0.12	0.38 +0.04	477.65+0.29	0.48 +0.06	820.70+0.32	0.70 +0.10	1213.7+0.6	0.21+0.08
171.10 +0.13	0.23 +0.02	484.49+0.30	1.4 +0.2	825.00+0.33	0.29 +0.05	1220.7+0.6	2.7 +0.5
174.84 +0.13	0.057+0.011	487.71+0.30	2.4 +0.3	829.65+0.33	0.83 +0.14	1227.1+0.6	0.94+0.17
175.65 +0.17	0.91 +0.15	494.60+0.60	0.16 +0.03	832.25+0.33	1.0 +0.2	1237.2+0.6	0.51+0.11
180.75 +0.17	0.70 +0.07	499.88+0.31	0.47 +0.07	836.70+0.33	0.32 +0.07	1253.6+0.6	0.56+0.11
185.25 +0.18	2.4 +0.3	504.60+0.31	0.62 +0.09	839.69+0.34	1.9 +0.3	1261.3+1.2	0.15+0.06
192.88 +0.19	2.7 +0.2	511.80+0.32	0.97 +0.13	843.54+0.34	0.69 +0.14	1270.0+0.6	0.81+0.17
196.48 +0.15	0.17 +0.02	515.00+0.32	0.88 +0.13	855.92+0.35	2.3 +0.3	1276.8+0.6	0.81+0.17
202.89 +0.16	0.055+0.008	519.90+0.33	3.0 +0.4	862.12+0.35	5.3 +0.9	1286.2+0.7	0.84+0.20
204.48 +0.16	0.17 +0.02	521.85+0.33	0.11 +0.04	866.29+0.35	0.44 +0.10	1290.7+0.7	0.56+0.14
217.10 +0.23	0.85 +0.08	527.94+0.33	0.37 +0.05	874.73+0.35	0.24 +0.06	1301.5+0.7	2.4 +0.4
223.12 +0.23	1.5 +0.1	536.51+0.34	0.078+0.017	877.93+0.36	1.2 +0.2	1313.8+0.7	1.4 +0.3
227.93 +0.24	0.70 +0.11	539.80+0.34	0.90 +0.13	884.02+0.36	0.30 +0.07	1325.0+0.7	0.40+0.12
229.38 +0.24	1.4 +0.2	544.78+0.35	0.10 +0.02	888.71+0.37	0.81 +0.13	1335.0+0.7	4.7 +1.0
236.21 +0.25	0.045+0.008	548.98+0.35	0.64 +0.13	893.55+0.37	0.54 +0.10	1340.6+0.7	2.0 +0.5
242.97 +0.21	0.90 +0.19	551.10+0.36	0.23 +0.05	897.85+0.37	0.57 +0.10	1346.7+0.7	1.1 +0.2
244.14 +0.21	0.48 +0.10	563.34+0.37	0.44 +0.08	903.21+0.37	0.33 +0.10	1351.8+0.7	0.73+0.24
251.18 +0.22	0.13 +0.01	566.28+0.37	1.5 +0.2	905.26+0.37	1.0 +0.2	1355.6+0.7	0.57+0.19
255.68 +0.23	1.8 +0.1	570.74+0.38	0.84 +0.13	909.75+0.38	1.7 +0.4	1363.5+0.7	2.4 +0.5
261.37 +0.23	0.084+0.011	578.28+0.38	3.6 +0.6	913.52+0.38	0.51 +0.11	1370.3+0.7	4.1 +1.1

TABLE I (Continued)

E_0 (eV)	$g\Gamma_n^0$ (meV)	E_0 (eV)	$g\Gamma_n^0$ (meV)	E_0 (eV)	$g\Gamma_n^0$ (meV)	E_0 (eV)	$g\Gamma_n^0$ (meV)
1375.9+0.7	6.2 +1.3	1729.2+0.5	0.26+0.12	2085.7+0.7	0.92+0.26	2532.3+0.9	3.6 +0.8
1383.0+0.7	0.24+0.11	1737.6+0.5	0.16+0.10	2093.2+0.7	2.8 +0.7	2550.8+0.9	2.2 +0.7
1389.5+0.7	1.5 +0.3	1739.1+0.5	0.22+0.12	2101.8+0.7	3.3 +0.9	2556.9+0.9	0.4 +0.2
1399.3+0.7	1.7 +0.4	1745.1+0.5	2.0 +0.5	2107.7+0.7	2.1 +0.5	2560.0+0.9	1.1 +0.4
1402.9+0.7	0.37+0.13	1747.1+0.5	0.55+0.24	2117.7+0.7	2.4 +0.7	2571.2+0.9	2.0 +0.5
1413.7+0.8	7.4 +1.6	1756.1+0.5	0.79+0.19	2126.7+0.7	3.0 +0.9	2579.2+0.9	0.59+0.19
1418.1+0.8	0.64+0.24	1761.7+0.5	1.0 +0.2	2135.1+0.7	0.43+0.17	2585.0+0.9	0.57+0.24
1430.2+0.8	0.93+0.19	1772.9+0.5	1.2 +0.3	2138.2+0.7	1.0 +0.4	2589.1+0.9	2.9 +0.9
1447.0+0.8	1.2 +0.2	1786.0+0.6	4.5 +0.9	2147.7+0.7	0.52+0.19	2600.3+1.0	6.9 +1.8
1461.5+0.8	5.8 +1.0	1797.7+0.6	0.27+0.09	2155.5+0.7	0.25+0.13	2615.5+1.0	1.1 +0.5
1477.7+0.8	0.38+0.11	1802.6+0.6	3.1 +0.7	2161.7+0.7	0.45+0.15	2619.8+2.0	1.2 +0.6
1483.9+0.8	3.0 +0.6	1816.8+0.6	1.8 +0.4	2169.3+0.7	2.1 +0.5	2630.6+1.0	1.3 +0.4
1491.0+0.8	0.30+0.10	1821.6+1.2	0.56+0.16	2175.5+0.7	1.1 +0.3	2654.7+1.0	0.91+0.31
1494.2+0.8	0.93+0.23	1831.8+0.6	3.3 +0.7	2178.3+1.4	1.3 +0.5	2658.1+1.0	0.50+0.23
1498.1+0.8	0.21+0.08	1838.5+0.6	0.21+0.12	2182.5+0.7	0.43+0.17	2666.6+1.0	2.4 +0.7
1510.5+0.8	1.0 +0.2	1842.6+0.6	0.35+0.14	2192.3+0.8	1.3 +0.3	2676.0+1.0	0.81+0.27
1535.3+0.9	7.1 +1.3	1847.2+0.6	1.9 +0.4	2205.0+0.8	1.1 +0.3	2683.6+2.0	1.1 +0.3
1545.7+0.9	2.1 +1.5	1859.7+0.6	1.9 +0.4	2207.5+0.8	0.36+0.17	2696.0+2.0	0.54+0.27
1551.9+0.9	2.2 +0.5	1869.6+0.6	0.24+0.08	2218.6+0.8	4.2+1.1	2702.7+1.0	2.3 +0.7
1561.2+0.9	0.61+0.23	1871.6+0.6	0.42+0.16	2228.6+0.8	3.4 +0.8	2711.4+1.0	2.1 +0.7
1565.4+0.9	1.5 +0.4	1874.7+0.6	0.24+0.09	2240.2+1.6	0.82+0.19	2717.2+1.0	4.4 +1.2
1568.2+0.9	2.3 +0.8	1881.3+0.6	0.55+0.18	2251.1+1.6	1.1 +0.3	2733.8+1.0	0.42+0.23
1575.1+0.9	2.7 +0.6	1885.3+0.6	4.1 +0.9	2260.3+0.8	2.7 +0.7	2737.2+2.0	0.59+0.32
1582.5+0.9	5.8 +1.3	1897.6+1.2	0.39+0.11	2265.8+0.8	2.9 +0.8	2746.6+1.0	1.2 +0.3
1587.2+0.9	3.3 +0.8	1905.0+0.6	1.8 +0.4	2278.0+0.8	0.44+0.25	2765.9+1.0	8.7 +1.9
1592.9+0.9	1.3 +0.5	1923.4+0.6	0.12+0.04	2281.4+0.8	1.4 +0.4	2777.0+1.0	0.93+0.34
1598.1+0.9	2.0 +0.5	1929.2+0.6	1.5 +0.4	2295.3+0.8	1.5 +0.5	2803.1+1.0	2.3 +0.6
1603.4+0.9	0.32+0.17	1932.0+0.6	1.5 +0.4	2299.4+0.8	0.44+0.19	2813.8+1.0	2.2 +0.7
1608.7+0.9	0.82+0.22	1942.8+0.6	0.57+0.16	2309.2+0.8	6.0 +1.5	2825.1+1.1	0.73+0.26
1614.9+0.9	1.2 +0.3	1948.4+0.6	0.84+0.23	2319.6+0.8	8.1 +2.3	2836.4+1.1	2.6 +0.8
1622.9+0.9	0.92+0.30	1952.6+0.6	0.37+0.14	2335.3+0.8	1.5 +0.4	2848.8+1.1	0.71+0.34
1626.0+0.9	0.42+0.22	1965.6+0.6	2.9 +0.7	2345.7+0.8	0.43+0.21	2853.6+1.1	0.64+0.32
1629.6+0.9	2.2 +0.6	1970.4+0.6	0.81+0.23	2347.7+0.8	0.58+0.25	2859.3+1.1	0.39+0.21
1634.6+0.9	0.37+0.17	1978.5+0.6	0.79+0.18	2368.1+0.8	1.0 +0.4	2864.5+1.1	0.52+0.24
1641.0+0.9	1.4 +0.4	1987.3+0.6	0.49+0.11	2370.8+0.8	0.82+0.33	2876.1+2.2	0.99+0.37
1644.1+1.0	0.76+0.25	1994.6+0.6	1.8 +0.5	2373.6+0.8	0.92+0.37	2884.6+1.1	0.82+0.30
1649.2+1.0	0.42+0.22	1997.0+0.6	3.4 +0.9	2430.8+0.9	2.1 +0.4	2893.1+1.1	2.1 +0.7
1659.7+1.0	0.26+0.12	2002.8+1.2	0.80+0.22	2440.7+0.9	3.8 +0.8	2924.2+1.1	0.27+0.28
1666.7+1.0	0.24+0.12	2014.2+0.7	3.1 +0.7	2453.1+0.9	3.6 +0.8	2931.3+1.1	0.74+0.37
1685.3+1.0	0.20+0.10	2023.5+0.7	0.47+0.16	2470.7+0.9	0.48+0.20	2935.6+1.1	2.0 +0.7
1694.3+1.0	0.23+0.09	2032.9+0.7	3.5 +0.9	2474.1+0.9	1.3 +0.5	2949.3+1.1	3.3 +1.1
1702.2+1.0	0.80+0.17	2047.4+0.7	1.7 +0.4	2478.8+0.9	1.1 +0.4	2953.4+1.1	2.0 +0.7
1709.7+1.0	0.23+0.12	2057.0+1.4	0.44+0.15	2490.6+0.9	1.0 +0.3	2969.1+1.2	1.7 +0.6
1714.1+0.5	1.3 +0.3	2064.7+0.7	1.8 +0.4	2494.9+0.9	0.25+0.11	2974.6+1.2	0.95+0.46
1717.5+0.5	0.15+0.07	2071.8+0.7	0.57+0.18	2510.7+1.8	0.40+0.24	2980.2+1.2	4.2 +1.5
1722.8+0.5	0.48+0.17	2076.3+0.7	0.31+0.18	2523.2+0.9	0.86+0.22	2984.7+1.2	0.51+0.29
1727.2+0.5	0.12+0.06	2077.9+0.7	0.39+0.22				

^{175}Lu . Flat detector transmission measurements were also made using ^{10}B at the 39.57 m detector for samples having $1/n=70.4$ and 702 b/atom. The 39.57 m data were mainly useful below 500 eV. In addition, we have measurements using the $1/n=70.4$ b/atom sample at the 39.57 m detector (for resonance capture γ rays) with and without the $1/n=702$ b/atom sample in transmission (self-indica-

tion) and also using the $1/n=702$ b/atom sample at the detector alone without transmission sample. About 2.2×10^6 total cyclotron bursts for ^{175}Lu samples were involved excluding "open" beam measurements. The thick sample ($1/n=70.4$ b/atom) was about 3.2×12.7 cm area and the thin sample ($1/n=702$ b/atom) about 6.4×12.7 cm area. The $^{175}\text{Lu}_2\text{O}_3$ samples contained a total of about

200 g of ^{175}Lu obtained on loan from the Isotope Division of Oak Ridge National Laboratory.

The preliminary analysis was the same as described for the Er isotopes.¹ For each resonance seen in each operating condition, we obtain an implied relation between $g\Gamma_n$ and Γ from an area analysis. For most of the lower energy levels ($E_0 < 500$ eV), this gave many intersecting curves for each resonance, thereby establishing $g\Gamma_n$ and, where favorable, Γ value, and thus $\Gamma_\gamma \approx \Gamma - 2g\Gamma_n$. At higher energies there was usually just a single curve from the 200 m transmission measurements. In that case, we used the intersection of that curve with the curve $\Gamma = 2g\Gamma_n + \langle\Gamma_\gamma\rangle$, using $\langle\Gamma_\gamma\rangle = 75$ meV. The results were not sensitive to small changes in Γ_γ for these levels or to the exact choice $g = \frac{7}{16}$ or $\frac{9}{16}$ if $\Gamma \approx \langle\Gamma_\gamma\rangle + (g\Gamma_n)/g$.

The results for the ($E_0, g\Gamma_n^0$) values for 446 levels in ^{175}Lu to 3 keV are given in Table I. We do not show the 40 individual Γ_γ values which give $\langle\Gamma_\gamma\rangle = 77$ meV. The individual values ranged from (59 ± 20) to (100 ± 20) meV. The true spread is probably smaller than that of our measured values, which had 31 between 70 and 85 meV.

III. SYSTEMATICS OF THE RESULTS

Figure 1 shows the cumulative level count N vs energy E . The initial slope, to 200 eV, corresponds to $\langle D_0 \rangle = 3.66$ eV followed by a relatively straight section having $\langle D_0 \rangle = 5.21$ eV to 1 keV, above which an increasing fraction of weak s levels are missed or improperly resolved. The $J=3$ and 4 s level sets are randomly merged with no level repulsion acting between levels of different J . Our analysis to determine the most probably true $\langle D_0 \rangle$ is given later.

Figure 2 shows the plot of $\sum g\Gamma_n^0$ vs E to 3 keV. The experimental plot stays surprisingly close to

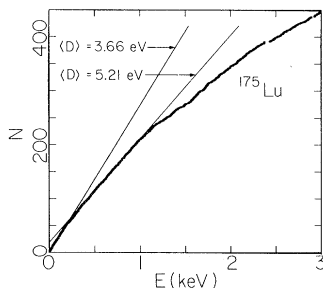


FIG. 1. Plot of the observed number N of levels seen in ^{175}Lu vs energy E to 3 keV. Since two $l=0$ populations are merged, level repulsion effects are small. The straight lines correspond to local slopes in terms of $\langle D \rangle$. A detailed analysis suggests that about 92, 72, 59, and 51% of the complete set of s levels in ^{175}Lu are included below 200 eV, 1 keV, 2 keV, and 3 keV, respectively.

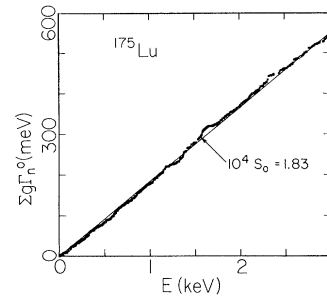


FIG. 2. Plot of $\sum g\Gamma_n^0$ vs E for levels in ^{175}Lu . The slope of the plot gives the s strength function S_0 . Such a plot is insensitive to missed weak s levels.

a slope corresponding to $10^4 S_0 = 1.83$. Such a plot is insensitive to missed weak levels. We choose as our final value $10^4 S_0 = (1.83 \pm 0.12)$.

Figure 3 shows a histogram of $(g\Gamma_n^0)^{1/2}$ values to 1 keV and its comparisons with three differently merged Porter-Thomas single channel distributions each normalized to $N=290$ to fit the upper part of the experimental distribution. Such a plot is used mainly as a test of missed weak s levels, or the presence of some p levels. In this case, it is unlikely that any p levels were seen; so the test is best used to estimate the number of missed weak s levels (first two histogram boxes) and thus the true $\langle D \rangle$ for s levels.

The comparison with the Porter-Thomas single channel distribution is complicated by the presence of merged $J=3$ and 4 s populations. We take the two level densities in the ratio of the $(2J+1)$ values, or $\frac{7}{9}$ for $J=3$ and $J=4$. Let $R \equiv$ the $\langle g\Gamma_n^0 \rangle$ ratio, or the S_0 ratio for the $J=4$ to $J=3$ separate

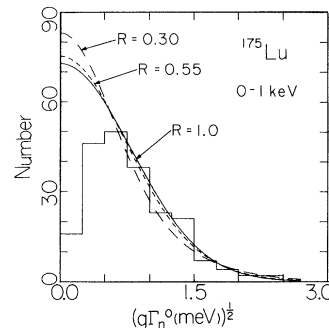


FIG. 3. Histogram of observed $(g\Gamma_n^0)^{1/2}$ values for ^{175}Lu to 1000 eV. It is expected that missed weak s levels will have $(g\Gamma_n^0)^{1/2}$ values corresponding to the first and second histogram boxes, so a fit is made to the upper part of the histogram based on two merged single channel Porter-Thomas distributions. The level densities for $J=3$ and $J=4$ are taken proportional to the $(2J+1)$ values. R is the ratio of S_0 for $J=4$ to that for $J=3$. The curves are normalized to 290 levels vs 209 observed levels and to $10^4 S_0 = 1.83$ for ^{175}Lu .

populations. The usual choice is $R=1$ in the absence of specific evidence to the contrary. Namenson, Stolovy, and Smith²² have assigned relative probabilities P_{j3} and P_{j4} that each of the 53 strongest levels in ^{175}Lu to 238 eV has $J=3$ or $J=4$. Using our $g\Gamma_n^0$ values for these levels, we obtain

$$R \approx \frac{\sum P_{j4}(g\Gamma_n^0/g_4)_j}{\sum P_{j3}(g\Gamma_n^0/g_3)_j} = (0.55 \pm 0.20),$$

which suggests a possible difference from $R=1$. The quoted uncertainty is mainly due to finite sample size. The comparison curves in Fig. 3 are for $N=290$ and $10^4 S_0 = 1.83$ for $R=1$, 0.55, and 0.3, respectively.

For each of these three R choices, we also calculated the expectation value for the number of weak s levels missed on the basis of our judgment of the threshold ($g\Gamma_n^0$) vs E for detection of weak s levels. The predicted numbers of missed weak s levels to 200 eV were 4.9, 5.1, and 5.6 for the choices $R=1.0$, 0.55, and 0.30, i.e., essentially five levels for reasonable choices of R . We therefore have $\langle D_0 \rangle = (3.45 \pm 0.15)$ eV for our final choice of the average s level spacing for ^{175}Lu . This is consistent with the above Porter-Thomas distribution fit to the upper part of $(g\Gamma_n^0)^{1/2}$ histogram for levels to 1 keV.

Figure 4 shows the histogram of nearest neighbor level spacings to 200 eV (52 spacings). The curve is the Wigner distribution for two merged populations, each having level density proportional to $(2J+1)$. The previous analysis suggests that five levels were missed to 200 eV, so five spacings should each be split into two smaller spacings. This probably accounts for the improbably large number of spacings in the last histogram

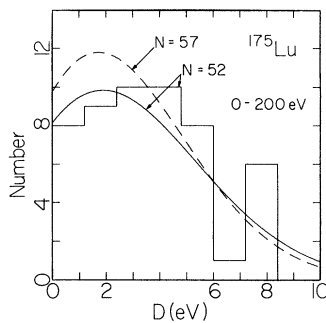


FIG. 4. Histogram of the nearest neighbor s level spacing distribution for ^{175}Lu to 200 eV. Since 5 weak s levels were probably missed, the significance of the comparison with the theoretical curve for two merged Wigner distributions was reduced. It probably explains the high histogram box near $D=8$ eV. Curves are shown for $N=52$ and 57 for level densities in the ratio 7 to 9.

box.

Before attempting to test for the probable approximate positions of the missed s levels, the Dyson-Mehta²³ Δ test was applied to the observed level set to 200 eV. Here Δ is the mean square deviation of the staircase plot of N vs E from a best fit straight line. The fit, shown in Fig. 5, gives $\Delta_{\text{exp}} = 0.49$ vs $\Delta_{\text{DM}} = 0.65 \pm 0.22$ for two merged populations of nearly equal densities, each obeying the statistical orthogonal ensemble (OE) theory.¹ The observed value $\rho = -0.23$ for the correlation coefficient for adjacent nearest neighbor spacings compares with the theoretical value $\rho = -(0.26 \pm 0.12)$ for this case.

The significance of the excellent agreement of the statistical parameters with those predicted for the OE theory is greatly reduced by the fact that we probably missed approximately five weak s levels to 200 eV.

We have made various tests as to approximately where the five missed weak levels to 200 eV should be situated. The Dyson F statistic test^{24, 25} for two merged populations with density ratio $= \frac{7}{5}$ suggests that no levels were missed to ~ 60 eV. If five levels are added at 65, 93, 134, 178, and 189 eV, at the centers of relatively large nearest neighbor spacings above 60 eV, the value of Δ becomes 0.32 and $\rho = -0.24$, with a proper reduction of the Dyson F test fluctuations.

A comparison of our level parameter results with those of the lower resolution results of Refs. 18 and 19 is only significant below ~ 60 eV. Our $\langle \Gamma_\gamma \rangle$ of 77 meV compares with $\Gamma_\gamma = (40 \pm 20)$, (160 ± 50) , (70 ± 20) , (90 ± 30) , and (80 ± 30) meV for levels at 11.20, 20.45, 23.42, 36.50, and 40.59

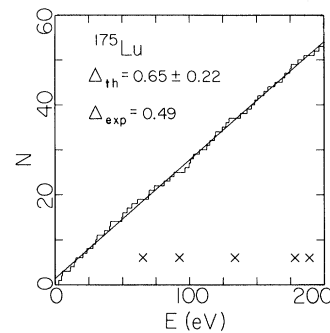


FIG. 5. Comparison of the staircase plot of number of observed levels, N , vs energy with the best fit straight line. The mean square deviation is the Dyson-Mehta Δ . For two merged orthogonal ensembles of nearly equal mean level density $\Delta_{\text{th}} = (0.65 \pm 0.22)$ for 53 levels, vs measured $\Delta = 0.49$. The excellence of the fit is made less significant by the fact that five weak s levels were probably missed in this energy interval. The \times indicates where the analysis, see text, suggests that these five levels may be situated (approximately).

eV in Ref. 19. A value (70.8 ± 1.5) meV of Γ_γ for the level at 2.58 eV vs our (77 ± 10) meV was obtained by Brunner and Widder.²⁶ A comparison of our $g\Gamma_n^0$ values with those of Refs. 18 and 19 shows fair agreement except that the ORNL values¹⁸ are generally larger than ours and the BNL values,¹⁹ particularly for the strong levels at 13.97, 23.42, 30.11, and 40.59 eV where their values are about 50 to 100% larger.

The s strength function, $10^4 S_0 = (1.83 \pm 0.12)$ for ^{175}Lu is about the same size as for adjacent nuclides,^{1, 4} and for that expected from the distorted nucleus optical model.²⁷

We wish to thank Dr. H. Ceulemans, Dr. H. S. Camarda, Dr. M. Slagowitz, and Dr. S. Wynchank for their involvement in the measurements.

† Work supported in part by the U. S. Atomic Energy Commission.

¹H. I. Liou *et al.*, Phys. Rev. C 5, 974 (1972), Er.

²F. Rahn *et al.*, Phys. Rev. C 6, 251 (1972), Sm, Eu.

³F. Rahn *et al.*, Phys. Rev. C 6, 1854 (1972), ²³²Th, ²³⁸U.

⁴H. I. Liou *et al.*, Phys. Rev. C 7, 823 (1973), Yb.

⁵H. S. Camarda *et al.*, Phys. Rev. C 8, 1813 (1973), W.

⁶F. Rahn *et al.*, Phys. Rev. C 8, 1827 (1973), Na.

⁷U. N. Singh *et al.*, Phys. Rev. C 8, 1833 (1973), K.

⁸H. I. Liou *et al.*, Phys. Rev. C 10, 709 (1974), Cd.

⁹G. Hacken *et al.*, Phys. Rev. C 10, 1910 (1974), In.

¹⁰F. Rahn *et al.*, Phys. Rev. C 10, 1904 (1974), Gd.

¹¹U. N. Singh *et al.*, Phys. Rev. C 10, 2138 (1974), Cl.

¹²U. N. Singh *et al.*, Phys. Rev. C 10, 2143 (1974), Ca.

¹³U. N. Singh, H. I. Liou, J. Rainwater, G. Hacken, and J. B. Garg, Phys. Rev. C 10, 2147 (1974), F.

¹⁴U. N. Singh, H. I. Liou, J. Rainwater, G. Hacken, and J. B. Garg, Phys. Rev. C 10, 2150 (1974), Mg.

¹⁵H. I. Liou, G. Hacken, J. Rainwater, and U. N. Singh, Phys. Rev. C 11, 462 (1974), Dy.

¹⁶H. I. Liou, J. Rainwater, G. Hacken, and U. N. Singh, Phys. Rev. C 11, 457 (1974), Ar.

¹⁷U. N. Singh, J. Rainwater, H. I. Liou, G. Hacken, and J. B. Garg, Phys. Rev. C 11, 1123 (1975), Al.

¹⁸R. C. Block, G. G. Slaughter, and J. A. Harvey, ORNL Report No. ORNL-2718, 1959 (unpublished), p. 26.

¹⁹J. A. Harvey, D. J. Hughes, R. S. Carter, and V. E. Pilcher, Phys. Rev. 99, 10 (1955).

²⁰*Resonance Parameters*, compiled by S. F. Mughabghab and D. I. Garber, Brookhaven National Laboratory Report No. BNL-325 (National Technical Information Service, Springfield, Virginia, 1973), 3rd ed., Vol. I.

²¹O. A. Wasson and R. E. Chrien, Phys. Rev. C 2, 675 (1970).

²²A. I. Namenson, A. Stolovy, and G. L. Smitii, in Proceedings of the Second International Symposium on Neutron Capture Gamma-Ray Spectroscopy and Related Topics, Petten, The Netherlands, September, 1974 (unpublished).

²³F. J. Dyson and M. L. Mehta, J. Math. Phys. 4, 701 (1963).

²⁴F. J. Dyson, private communication.

²⁵H. I. Liou, H. S. Camarda, and F. Rahn, Phys. Rev. C 5, 1002 (1972).

²⁶J. Brunner, F. Widder, Report No. EIR-123, 1967 (unpublished); also in *Proceedings of the Conference on Nuclear Data, Microscopic Cross Sections and Other Data Basic for Reactors, Paris, 1966* (International Atomic Energy Agency, Vienna, Austria, 1967), paper CN-23/20.

²⁷D. M. Chase, L. Wilets, and A. R. Edmunds, Phys. Rev. 110, 1080 (1958).